

# Hydrothermal and post-heat treatments of $\text{TiO}_2/\text{ZnO}$ composite powder and its photodegradation behavior on methyl orange

Xingming Xu, Jianfei Wang, Jintao Tian<sup>\*</sup>, Xin Wang, Jinhui Dai, Xiaoyun Liu

*Institute of Materials Science and Engineering, Ocean University of China, Songling Road 238, Qingdao 266100, PR China*

Received 15 November 2010; received in revised form 5 December 2010; accepted 4 March 2011

Available online 14 April 2011

## Abstract

The composite powder of  $\text{TiO}_2/\text{ZnO}$  with an atomic ratio of Ti to Zn of 3/1 was prepared through sol–gel process followed by hydrothermal and post-heat treatments. The as-prepared powder was characterized in detail by means of XRD, TG/DTA, DLS, and SEM. The XRD results showed that by applying the hydrothermal process the crystallinity of the composite powder was significantly improved. The SEM and DLS results revealed no visible variations on particle morphology and size owing to the hydrothermal and post-heat treatments. The enhancement of the photocatalytic activity of the composite powder evaluated through methyl orange (MO) degradation under UV light irradiation was, therefore, attributed to its high crystallinity that was achieved during the hydrothermal process under a rather low temperature.

© 2011 Elsevier Ltd and Techna Group S.r.l. All rights reserved.

**Keywords:** B. Composites; Sol–gel chemistry; X-ray diffraction; Catalytic properties; Hydrothermal

## 1. Introduction

Because it have shown the merits of non-toxic, stable in aqueous solution, low cost, and environmentally friendly, titanium dioxide ( $\text{TiO}_2$ ) is well-known semiconductor with excellent photocatalytic property that has been widely used in improving environmental pollutants, antibacterial dopes, self-clean building, and so on [1–4]. However, the material presents a major drawback during the photocatalytic process: the relatively low value of the overall quantum efficiency due to the high recombination rate of photo-induced electron–hole pairs at or near its surface [5–7]. Some success in enhancing the photocatalytic activity has been conducted by several methods such as using nano-sized semiconductor crystallites instead of bulk materials [8], modifying photocatalysts by doping with ions [9–12], or coupling  $\text{TiO}_2$  to other oxides [13,14], for instance to zinc oxide (ZnO) for its characteristics of non-toxic and low cost [15,16]. Coupled semiconductor photocatalyst of  $\text{TiO}_2/\text{ZnO}$  has been investigated to enhance the photodegradation efficiency of  $\text{TiO}_2$  catalyst by a number of researchers and

its effect for improving photocatalytic efficiency was reported [17,18].

In our previous study the photocatalytic behavior of the  $\text{TiO}_2/\text{ZnO}$  composite has been studied [19]. It was found that even calcined at 500 °C the composite was rather amorphous. High crystallinity for the composite has been achieved by calcining the powder at higher temperature, for instance at 700 °C [20]. However, unexpected chemical reaction of  $\text{TiO}_2$  with ZnO to form  $\text{ZnTiO}_3$  was extensively occurred at this temperature in our study that has actually been applied by several researches for synthesis of  $\text{ZnTiO}_3$  powder [21–23]. On the other hand, it is known that hydrothermal treatment can improve the crystallinity of a powder at rather low temperature [3]. Since the crystallinity of a  $\text{TiO}_2$  or its composite catalyst can significantly influence its photocatalytic activity, the hydrothermal treatment may be a feasible way to enhance photocatalytic activity by improving the crystallinity of the  $\text{TiO}_2/\text{ZnO}$  composite powder. So, in this study we would like to conduct an investigation on the hydrothermal treatment of the  $\text{TiO}_2/\text{ZnO}$  composite powder and its effect on photocatalytic activity of the powder. The composite powder was prepared via sol–gel process followed by hydrothermal and post-heat treatments under various conditions. The as-prepared  $\text{TiO}_2/\text{ZnO}$  powder was characterized in detail and its photocatalytic activity was finally assessed.

<sup>\*</sup> Corresponding author. Tel.: +86 532 66781690; fax: +86 532 66781320.

E-mail address: [jttian@ouc.edu.cn](mailto:jttian@ouc.edu.cn) (J. Tian).

## 2. Experimental procedure

In the present study the  $\text{TiO}_2/\text{ZnO}$  composite powder was prepared via sol–gel process followed by hydrothermal and post-heat treatments. The preparation of  $\text{TiO}_2/\text{ZnO}$  sol has been reported elsewhere [20]; therefore, it is only briefly described here. The  $\text{TiO}_2/\text{ZnO}$  composite sol was achieved via directly mixing of the acidic  $\text{TiO}_2$  sol and the  $\text{ZnO}$  sol. The tetrabutyl titanate (Aldrich, 99.99%, TBT) was used as a precursor to prepare a precursor solution. A mixture of distilled water, glacial acetic acid, and ethanol was then dropped into the precursor solution at a speed of one drop per second under a strong stirring. After that, the solution was continuously stirred for 1 h to achieve a yellow transparent  $\text{TiO}_2$  sol. The zinc acetate (Aldrich, 99.99%) used as a precursor was dissolved in ethanol and stirred for at  $50^\circ\text{C}$  in water bath to get a precursor solution. A mixture of distilled water, diethanolamine, and ethanol was then dropped into the precursor solution at a speed of one drop per second under a strong stirring for half an hour. After that, the mixture of distilled water and ethanol was dropped into the precursor solution under a strong stirring for 2 h to achieve a transparent  $\text{ZnO}$  sol. The prepared  $\text{ZnO}$  sol was then directly incorporated into the  $\text{TiO}_2$  sol at an atomic molar ratio of Ti to Zn of 3/1 to achieve the  $\text{TiO}_2/\text{ZnO}$  composite sol. The mixture of  $\text{TiO}_2/\text{ZnO}$  sol was aged for a period of time at room temperature until it became gel. The gel was dried and pulverized to be powder. The gel powder was then transferred into a Teflon-lined autoclave and heated at various temperatures for different time. After hydrothermal treatment, the powder was washed with distilled water and dried. The powder was finally post-heat treated by calcination in air for 1 h in a muffle oven.

The as-prepared  $\text{TiO}_2/\text{ZnO}$  composite powder was characterized in detail as follows. The crystalline phase of  $\text{TiO}_2/\text{ZnO}$  powders was identified through X-ray diffraction (XRD, Model D8 Advance, BRUKER/AXS, Germany) method. The thermal decomposition behavior of the composite powder at high temperature was analyzed by thermo-gravimetric analyzer (TGA, ZRY-2P, Shanghai Precision and Scientific Instrument Co. Ltd., China) in air from room temperature to  $1000^\circ\text{C}$  at a heating rate of  $10^\circ\text{C}/\text{min}$ . The particle size and its distribution of the powder were quantitatively determined through dynamic light scattering (DLS, MPT-2, MALVERN, England) method. The particle morphology was observed using scanning electron microscopy (SEM, Model JSM-6700F, JEOL, Japan).

The photocatalytic performance of the as-prepared  $\text{TiO}_2/\text{ZnO}$  composite powder was assessed from the photodegradation of methyl orange (MO) solution using the powder as catalyst under UV irradiation. It was carried out as below. A MO solution with a concentration of  $0.025\text{ mmol/L}$  was prepared as an initial solution. The  $0.1\text{ g}$  composite powder was well pulverized in a quartz mortar and then incorporated into a  $200\text{ ml}$  initial MO solution to achieve a powder/solution suspension. The suspension was then UV irradiated using a  $20\text{ W}$  UV lamp having a wave length of  $254\text{ nm}$  for a period of reaction time. During the process the suspension was kept stirring. After reaction, the composite particles in the suspension were well filtered using a centrifugal filter. The filtrate of MO solution was then obtained

and its concentration was determined by measuring the absorbance at  $465\text{ nm}$  using a UV–vis spectrophotometer.

## 3. Results and discussion

### 3.1. Particle crystallization of the composite powder

In order to clarify the effect of hydrothermal treatment on the particle crystallization and phase composition, the  $\text{TiO}_2/\text{ZnO}$  composite powder was hydrothermally treated under various conditions. The proposed temperature and time were as follows:  $120^\circ\text{C}$  for 1 h,  $150^\circ\text{C}$  for 24 h,  $180^\circ\text{C}$  for 24 h,  $200^\circ\text{C}$  for 12 h,  $200^\circ\text{C}$  for 24 h, and  $200^\circ\text{C}$  for 48 h. The XRD measurements were conducted on the untreated and hydrothermal treated powders and the results were shown in Fig. 1. As seen from Fig. 1, the untreated powder did not show any diffraction peak, indicating an amorphous state of the  $\text{TiO}_2/\text{ZnO}$  gel. After 1 h hydrothermal treatment at  $120^\circ\text{C}$ , visible diffraction peaks with low intensities were present. The powder was therefore partially crystallized under such condition, though the treating time was rather short. Significant crystallization of the composite powder can be achieved by applying the powder at  $150^\circ\text{C}$  for 24 h, as revealed by sharp peaks in Fig. 1 that was corresponding to anatase phase of  $\text{TiO}_2$ . No peak can be related to  $\text{ZnO}$ . Hydrothermal treatments at temperature higher than  $150^\circ\text{C}$  for a time longer than 24 h led to similar diffraction patterns. Thus, from an economic point of view the experimental parameters of  $150^\circ\text{C}$  and 24 h for hydrothermal process were preferred.

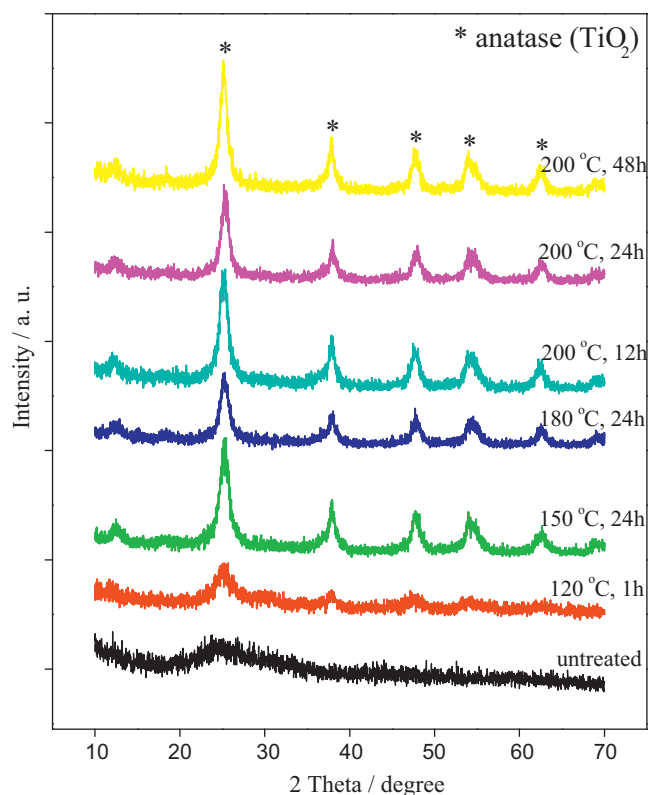


Fig. 1. XRD patterns of the  $\text{TiO}_2/\text{ZnO}$  composite powder untreated and hydrothermally treated at various temperatures for different times.

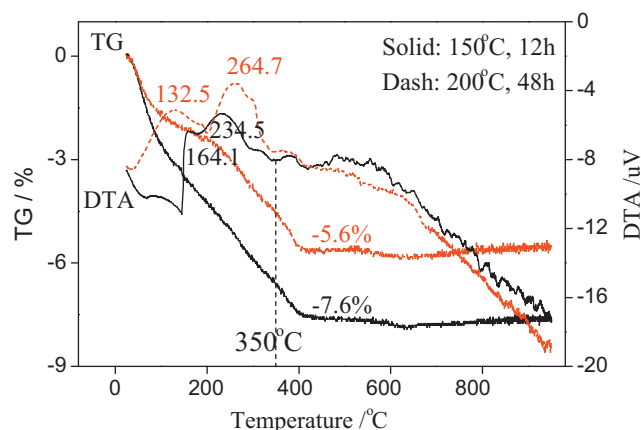


Fig. 2. TG/DTA curves of the  $\text{TiO}_2/\text{ZnO}$  composite powder (heating speed of  $10^\circ\text{C}/\text{min}$ ).

Before post-heat treatment, a TG/DTA analysis was conducted on the  $\text{TiO}_2/\text{ZnO}$  composite powder to determine the calcining temperature. The composite powders with hydrothermal treatments at  $150^\circ\text{C}$  for 24 h and at  $200^\circ\text{C}$  for 48 h were used as specimens. The derived TG/DTA curves were illustrated in Fig. 2. As seen from Fig. 2, two endothermic DTA peaks were observed at  $164.1^\circ\text{C}$  and  $234.5^\circ\text{C}$  for the powder hydrothermally treated at  $150^\circ\text{C}$  for 24 h. The weight loss was mainly occurred at a temperature range of  $150\text{--}400^\circ\text{C}$  while in the temperature range of  $400\text{--}1000^\circ\text{C}$  the TG curve was rather flat, giving a final total weight loss of 7.6%. The endothermic DTA peaks for the powder hydrothermally treated at  $200^\circ\text{C}$  for 48 h were at  $132.5^\circ\text{C}$  and  $264.7^\circ\text{C}$  and the resultant weight loss temperature range were  $200\text{--}400^\circ\text{C}$ . The final total weight loss of 5.6% was slightly smaller than that of the powder treated at  $150^\circ\text{C}$  for 24 h, which could be probably due to the better dissolution of organic components during the longer hydrothermal process of 48 h. Since the weight loss of the composite powder can be well achieved below  $400^\circ\text{C}$ , as shown in Fig. 2, a post-heat treating temperature of  $350^\circ\text{C}$  was therefore applied for the  $\text{TiO}_2/\text{ZnO}$  composite powder.

The  $\text{TiO}_2/\text{ZnO}$  composite was post-heat treated at  $350^\circ\text{C}$  for 1 h and its crystallization behavior during this process was examined through XRD. The results were shown in Fig. 3. As seen from Fig. 3, the composite powder calcined at  $350^\circ\text{C}$  for 1 h was in an amorphous state, in good agreement with our previous study where even with 2 h calcination at temperature as high as  $500^\circ\text{C}$  the composite was amorphous that has been attributed to the particle interactions of  $\text{TiO}_2$  and  $\text{ZnO}$  during the calcining process [19]. With a hydrothermal treatment at  $150^\circ\text{C}$  for 24 h, the composite powder, however, crystallized very well. Strong diffraction peaks were present in the patterns, corresponding to anatase phase of  $\text{TiO}_2$ . With hydrothermal treatment followed by calcination the obtained XRD patterns for the composite showed strong diffraction peaks and was essentially comparable to those of hydrothermally treated. Such results suggested that the hydrothermal process played a key role on the particle crystallization. High crystallinity has been achieved for the  $\text{TiO}_2/\text{ZnO}$  composite via hydrothermal treatment in our study.

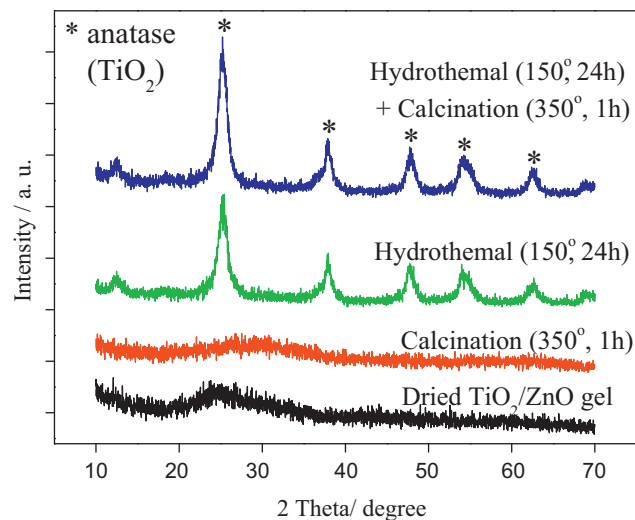


Fig. 3. XRD patterns of the  $\text{TiO}_2/\text{ZnO}$  composite powder after hydrothermal treatment and calcination at various temperatures for different times.

### 3.2. Particle morphology and size of the composite powder

The particle morphology of the  $\text{TiO}_2/\text{ZnO}$  composite was examined through SEM and the results were shown in Fig. 4. As seen from Fig. 4A–D, the composite powders at low magnification were small. The observations at high magnification showed presences of both large and small particles for the composites (Fig. 4a–d). The SEM results in Fig. 4 did not show any visible variation regarding particle shape, surface toughness, and size between the composites. This suggested that the hydrothermal treatment as well as the calcining process did not give a significant effect on the particle morphology of the  $\text{TiO}_2/\text{ZnO}$  composite.

Although from a SEM point of view no visible variation of particle size could be recognized in Fig. 4, quantitative determination of the particle size for the  $\text{TiO}_2/\text{ZnO}$  powder was quite essential. The particles size and its distribution of the powder were measured through DLS method. The composite powder was dispersed into a mixture of water and glycerin (volume ratio of water to glycerin of 2/3) under a strong stirring. The measurements were conducted and the results were shown in Table 1. As seen from Table 1, only one peak was present in the DLS results, giving a normal distribution of particle size. The derived Z-average diameters were in nano scale and comparable to each other for the composites prepared under different conditions. Such results suggested that the hydrothermal treatment as well as the calcining process did not noticeably affect the particle growth, in good agreement with the SEM results given above.

### 3.3. Photodegradation performance of the composite powder

The photocatalytic performance of the  $\text{TiO}_2/\text{ZnO}$  composite powder was explored via photodegradation of MO solution under UV irradiation using the powder as catalyst. The reaction time for photodegradation was scheduled to be 0 h, 0.5 h, 1 h,



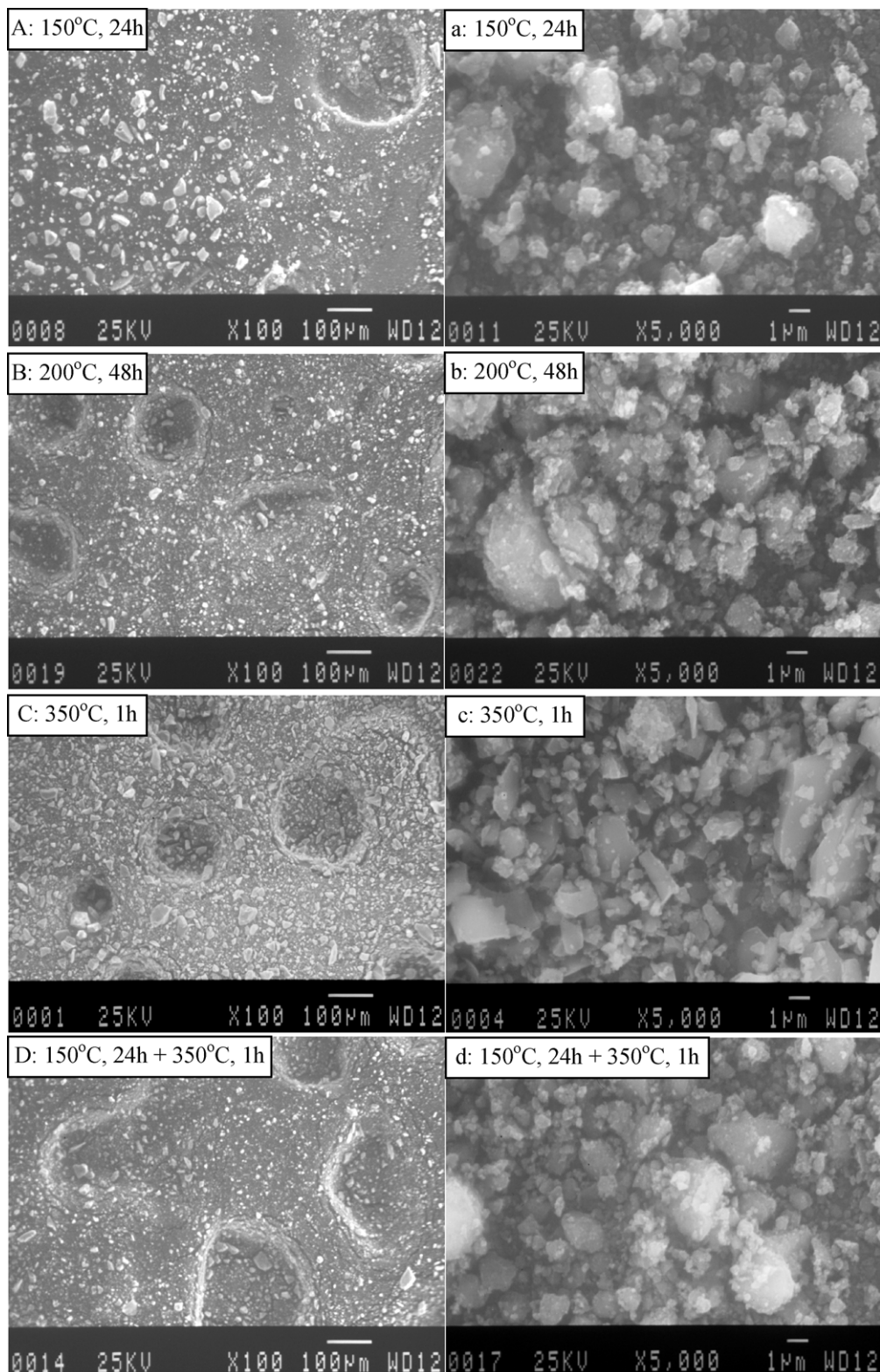


Fig. 4. SEM morphologies (A–D at low magnification and a–d at high magnification) of the  $\text{TiO}_2/\text{ZnO}$  composite powder after hydrothermal and calcining treatments.

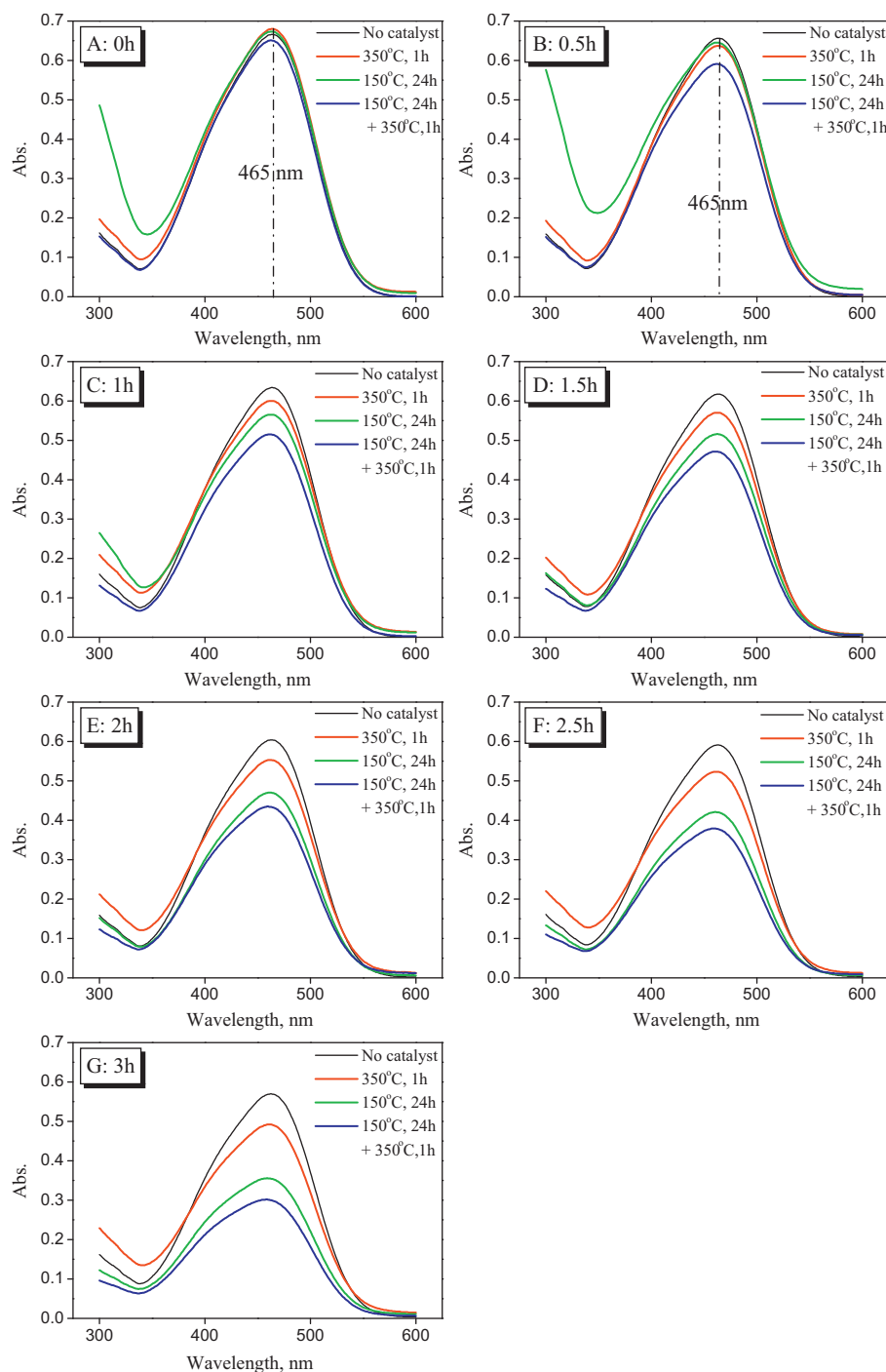
1.5 h, 2 h, 2.5 h and 3 h. By applying the composite powder as catalyst, the photodegradation process was conducted. Fig. 5 showed UV–vis adsorption spectra (A–G for different reaction time) of MO solution catalyzed by the  $\text{TiO}_2/\text{ZnO}$  composite powder under UV irradiation. As seen, all the curves in Fig. 5

showed absorption peaks with peak heights as maximum values at a wavelength of 465 nm. These maximum values remarkably decreased with the increase of the reaction time from 0.5 h to 3 h. In particular, the curves for the composite powder hydrothermally treated at 150 °C for 24 h were rather low in

Table 1

Results of particle size analysis of the TiO<sub>2</sub>/ZnO composite powder through DLS method.

Parameters for preparation	Peak 1		Peak 2		Z-average (nm)
	Diameter (nm)	Volume (%)	Diameter (nm)	Volume (%)	
Dried gel	154.4	100	0	0	207.2
350 °C, 1 h	527.4	100	0	0	543.5
150 °C, 24 h	413.0	100	0	0	446.3
200 °C, 48 h	516.1	100	0	0	603.3
150 °C, 24 h + 350 °C, 1 h	429.0	100	0	0	497.5

Fig. 5. UV-vis adsorption spectra (A–G for different reaction time) of MO solution catalyzed by the TiO<sub>2</sub>/ZnO composite powder under UV irradiation.

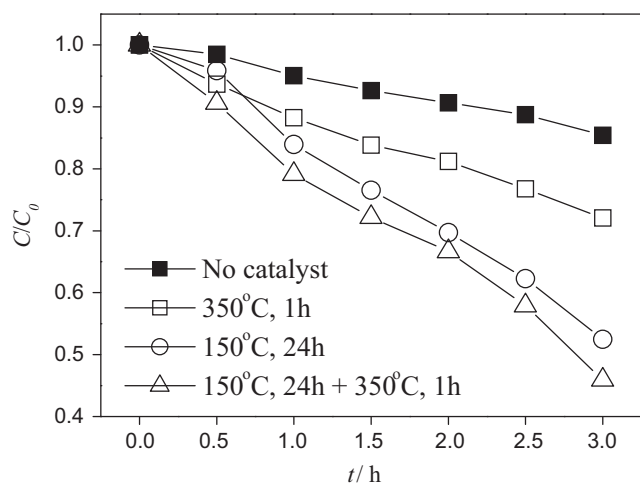


Fig. 6. Relationship between  $C/C_0$  and reaction time  $t$  for MO decomposition catalyzed by the  $\text{TiO}_2/\text{ZnO}$  composite powder under UV irradiation. The  $C$  and  $C_0$  were the concentration of MO solution at time  $t = t$  and  $t = 0$ , respectively.

each graph in Fig. 5 while those of hydrothermally treated followed by post-heat treatment were lowest.

In order to well understand the dynamic photodegradation behavior of the composite powder, the photodegradation efficiency of  $C/C_0$  was determined [20]. The depictive plots of  $C/C_0$  against reaction time  $t$  were shown in Fig. 6. As seen, the  $C/C_0$  for MO solution catalyzed by the composite powder post-heat treated at 350 °C for 1 h was lower than that of no catalyst. This suggested that MO has been degraded to some extent by the amorphous  $\text{TiO}_2/\text{ZnO}$  composite powder. By applying hydrothermal treatment at 150 °C for 24 h the composite catalyst significantly decomposed MO. The derived  $C/C_0$  curve was remarkably lower than that of the post-treated composite powder. The  $C/C_0$  for MO solution catalyzed by the composite powder hydrothermally treated followed by post-heat process was slightly lower than that of the composite only hydrothermally treated. Such results suggested that the photodegradation efficiency of the composite powder has been enhanced mainly via the hydrothermal treating process.

From above researches it was found that the photodegradation behavior of the  $\text{TiO}_2/\text{ZnO}$  composite powder was strongly related to the particle crystallization of the powder. It has been reported that the photocatalytic activity of  $\text{TiO}_2$  catalyst is dependent on both crystallinity and specific surface area of the material [24]. In this study by applying hydrothermal treatment the crystallinity of the composite powder was significantly improved. Both the SEM and DLS results revealed no visible effects of the process on the particle morphology and size. As a result, the enhancement of the photodegradation efficiency of the composite powder was attributed to its high crystallinity that was achieved during the hydrothermal process.

#### 4. Conclusion

The  $\text{TiO}_2/\text{ZnO}$  composite powder with an atomic molar ratio of Ti to Zn of 3/1 has been prepared via sol–gel process followed by hydrothermal and post-heat treatments. The

crystallinity of composite powder was significantly improved through hydrothermal treatment at rather low temperature. There were no visible variations on particle morphology and size owing to the hydrothermal process. Thus, the enhanced photodegradation efficiency was achieved by improving the crystallinity of the  $\text{TiO}_2/\text{ZnO}$  composite powder through hydrothermal treatment.

#### Acknowledgements

This work was financially supported by Specialized Research Fund for the Doctoral Program of Higher Education (SRFDP, 200804231004) and Shandong Province Middle-aged and Young Scientists Research Incentive Fund (BS2009CL016). The authors were also grateful to Prof. Zhibin Zhu, Prof. Jinshan Tan, Dr. Feng Sun, and Dr. Hongfen Wang for supports of DLS, SEM, XRD & TGA, UV–vis measurements.

#### References

- [1] J.J. Wu, C.H. Tseng, *Appl. Catal. B* 66 (2006) 51.
- [2] Y.W. Wang, L.Z. Zhang, K.J. Deng, X.Y. Chen, Z.G. Zou, *J. Phys. Chem. C* 111 (2007) 2709.
- [3] A.A. Aal, M.A. Barakat, R.M. Mohamed, *Appl. Surf. Sci.* 254 (2008) 4577.
- [4] L. Jing, B. Xin, F. Yuan, B. Wang, K. Shi, W. Cai, H. Fu, *Appl. Catal. A: Gen.* 275 (2004) 49.
- [5] K. Tennakone, P.K.M. Bandaranayake, P.V.V. Jayaweera, A. Konno, G.R.R.A. Kumara, *Physica E* 14 (2002) 190.
- [6] M. Ni, M.K.H. Leung, D.Y.C. Leung, K. Sumathy, *Renew. Sust. Energy Rev.* 11 (2007) 401.
- [7] G.K. Mor, O.K. Varghese, M. Paulose, K. Shankar, C.A. Grimes, *Sol. Energy Mater. Sol. Cells* 90 (2006) 2011.
- [8] K. Arshak, J. Corcoran, O. Korostynska, *Sens. Actuators A* 123 (124) (2005) 194.
- [9] J. Keleher, J. Bashant, N. Heldt, L. Johnson, Y.Z. Li, *World J. Microbiol. Biotechnol.* 18 (2002) 133.
- [10] L. Diamandescu, F. Vasiliu, D.T. Mihaila, M. Feder, A.M. Vlaicu, C.M. Teodorescu, D. Macovei, *Mater. Chem. Phys.* 112 (2008) 146.
- [11] T.A. Tong, J.L. Zhang, B.Z. Tian, F. Chen, D.N. He, *J. Hazard. Mater.* 155 (2008) 572.
- [12] E.V. Skorb, L.I. Antonouskaya, N.A. Belyasova, D.G. Shchukin, H.M. Hwald, D.V. Sviridov, *Appl. Catal. B: Environ.* 84 (2008) 94.
- [13] K.Y. Jung, S.B. Park, *Mater. Lett.* 58 (2004) 2897.
- [14] H. Sayilkan, *Appl. Catal. A: Gen.* 319 (2007) 230.
- [15] A.A. Khodja, T. Sehili, J.F. Pilichowski, P. Boule, *J. Photochem. Photobiol. A: Chem.* 141 (2001) 231.
- [16] H.G.E. Shobaky, A.S. Ahmed, N.R.E. Radwan, *Colloids Surf. A: Physicochem. Eng. Aspects* 274 (2006) 138.
- [17] M.A. Aramendy, V. Borau, J.C. Colmenares, A. Marinas, J.M. Marinas, J.A. Navá, F.J. Urbano, *Appl. Catal. B: Environ.* 80 (2007) 88.
- [18] W.J. Zhang, S.L. Zhu, Y. Li, F.H. Wang, *Vacuum* 82 (2008) 328.
- [19] J.T. Tian, L.J. Chen, J.H. Dai, X. Wang, Y.S. Yin, P.W. Wu, *Ceram. Int.* 35 (2009) 2261.
- [20] J.T. Tian, J.F. Wang, J.H. Dai, X. Wang, Y.S. Yin, *Surf. Coat. Technol.* 204 (2009) 723.
- [21] L.Q. Wang, H.M. Kang, D.F. Xue, C.H. Liu, *J. Cryst. Growth* 311 (2009) 611.
- [22] Y.S. Chang, Y.H. Chang, I.G. Chen, G.J. Chen, Y.L. Chai, T.H. Fang, S. Wu, *Ceram. Int.* 30 (2004) 2183.
- [23] Z.C. Liu, D.X. Zhou, S.P. Gong, H. Li, *J. Alloys Compd.* 475 (2009) 840.
- [24] K. Cassiers, T. Linssen, M. Mathieu, Y.Q. Bai, H.Y. Zhu, P. Cool, E.F. Vansant, *J. Phys. Chem. B* 108 (2004) 3713.